REAL AND VIRTUAL PHOTON STRUCTURE AT HERA

DORIAN KCIRA
University of Wisconsin
ZEUS/DESY, Notkestrasse 85, 22607 Hamburg, Germany
dorian.kcira@desy.de

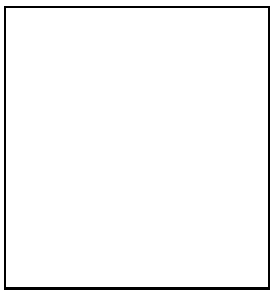

The structure of real and virtual photons has been studied in ep collisions at HERA using dijet production. Measurements of differential dijet cross sections as function of the fraction of photon's momentum invested in the dijet system are presented. The dependence of the cross sections on the virtuality of the photon and mean transverse energy squared of the two leading jets has been investigated. QCD calculations based on current parametrizations of the real and virtual photon parton distribution functions have been compared to the data.

1 Structure of Real Photons

Interactions of the real photon ($Q^2 \simeq 0$) have a two-component nature in leading order (LO) perturbative QCD (pQCD). Thus, two types of hard processes contribute in photon-proton interactions: in direct photon processes the entire momentum of the photon takes part in the hard subprocess with a parton from the proton, whereas in resolved photon processes the photon acts as a source of partons and one of these, carrying a fraction x_γ of the photon's momentum, enters the hard subprocess. Both LO processes can result in the production of two outgoing partons of large transverse energy that turn into two jets in the final state. In resolved photon processes, the photon structure is commonly described via parton distribution functions (PDFs) that receive contributions from both perturbative and non-perturbative terms. The fraction of photons momentum entering the hard interaction is evaluated using jets variables [1]:

$$x_\gamma^{\rm obs} = \frac{E_T^{{\rm jet},1} {\rm e}^{-\eta^{{\rm jet},1}} + E_T^{{\rm jet},2} {\rm e}^{-\eta^{{\rm jet},2}}}{2yE_e} \qquad (1)$$

The H1 Collaboration has determined LO effective parton densities of the photon [2] from the measurement of the dijet cross section $d\sigma/d\log(x_\gamma^{\rm obs})$. Dijet events were identified using a

cone algorithm with radius $R = 0.7$ and selected with jet transverse energies $E_T^{\rm jet} > 6$ GeV (after pedestal subtraction) and jet pseudorapidities $|\eta_{\rm jet,1} - \eta_{\rm jet,2}| < 1$, $\eta_{\rm jet} > -0.9 - \ln(x_\gamma^{\rm obs})$. The GRV92 LO parametrizations of the proton and photon PDFs [3] were used. An unfolding procedure [4] was used for extracting the effective parton distributions of the photon: $f_{\gamma,\rm eff} = q(x_\gamma) + \overline{q}(x_\gamma) + 9/4 g(x_\gamma)$. The effective parton density in the photon is adjusted to get the best agreement with the measured $x_\gamma^{\rm obs}$ distribution, having subtracted the LO QCD expectation for the direct photon contribution, as given by Monte Carlo (MC) simulation. The measured effective PDF of the photon is shown in figure 1. The contribution of quarks plus antiquarks in the photon as given by the GRV92 parametrization is shown separately and describes the data well at the highest values of x_γ but falls far below the data at low x_γ. Within the LO QCD the difference can only be attributed to a gluon contribution which is shown to rise strongly towards low x_γ. The gluon density was then extracted by subtracting the quark-antiquark contribution as predicted by the GRV92 parametrizations from the extracted effective parton density (right plot in 2).

The ZEUS Collaboration has measured dijet differential cross sections $d\sigma/dx_\gamma^{\rm obs}$ and compared them to NLO QCD calculations. Dijet events were identified with the k_T-cluster algorithm and selected with $E_T^{\rm jet,1} > 14$ GeV, $E_T^{\rm jet,2} > 11$ GeV and $-1 < \eta^{\rm jet} < 2$. The cross section was measured in the kinematic region $Q^2 < 1$ GeV^2 and inelasticity $0.20 < y < 0.85$. The measured differential cross section is shown in figure 2 in four ranges of $E_T^{\rm jet,1}$. The data are compared to NLO QCD calculations [5] that use the AFG-HO [6] (CTEQ4M [7]) parametrization for the PDFs of the photon (proton). The data are presented at the hadron level and compared to the calculations at the parton level. The effect of hadronisation has been evaluated to be $10 - 15\%$ using the Herwig [8] and Pythia [9] MC programs.

For all regions of $E_T^{\rm jet,1}$, the data at high $x_\gamma^{\rm obs}$ are reasonably well described by the calculation. However, for $x_\gamma^{\rm obs} < 0.8$ the data are always above the NLO prediction, most significantly in the higher $E_T^{\rm jet,1}$ regions. The percentage difference between data and NLO calculation is also shown in figure 2. The data lie $50 - 60\%$ above the NLO calculation for $E_T^{\rm jet} > 17\ GeV$; this discrepancy is larger than the uncertainties of the measurement and the estimation of the scale uncertainty in the NLO calculation. The data therefore suggest inadequencies in the current parametrization used for describing the structure of the photon. The use of the data in future fits would greatly improve our understanding of the photon PDFs.

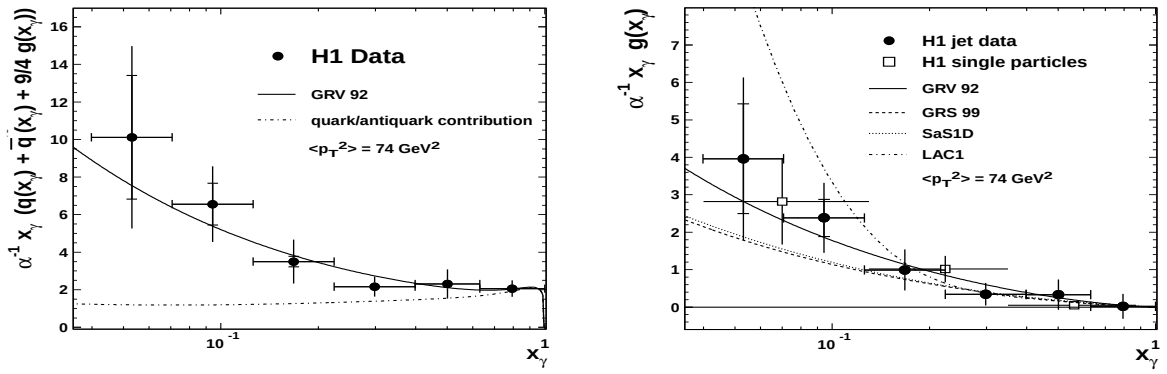

Figure 1: Effective parton distribution (left plot) and gluon distribution (right plot) of the photon multiplied by $\alpha^{-1}x_\gamma$ as a function of x_γ. The inner error bars give the statistical error only and the outer error bars the total error. LO parametrizations of PDFs based on fits to γ-γ data are also shown.

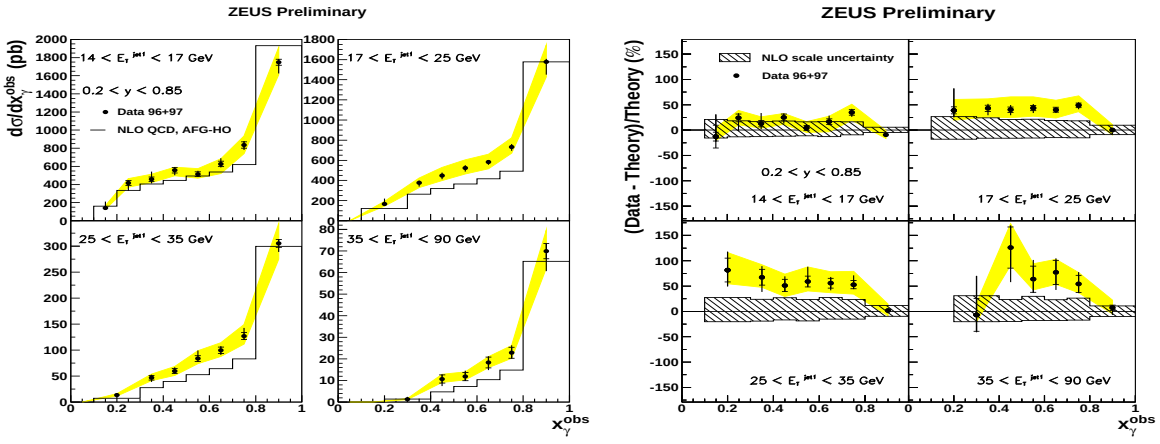

Figure 2: Differential dijet cross section $d\sigma/dx_\gamma^{\rm obs}$ in different ranges of the transverse energy of the jet with the highest $E_T^{\rm jet}$, $E_T^{\rm jet,1}$ (left plot). The data points are shown with statistical errors (inner bars) and systematic errors added in quadrature (outer bars). The energy scale uncertainty is shown as a shaded band. NLO QCD calculations which use the AFG-HO photon PDFs (histograms) are compared to the data. The percentage differences between the data and the NLO QCD calculations are also shown (right plot).

2 Structure of Virtual Photons

As the photon virtuality becomes non-zero, the non-perturbative contributions to the photon PDFs are expected to diminish. In this region, the language of photon PDFs may still be retained in describing processes where the virtual photon splits into a $q\bar{q}$ pair before interacting with the proton. However, the virtual photon PDFs are in principle calculable in pQCD. QCD predicts that for $(\overline{E_T})^2 > Q^2$, the virtual photon PDFs should decrease logarithmically as Q^2 grows [a].

Dijet events are selected in the $\gamma^* p$ frame with $E_T^{\rm jet,1} > 7.5$ GeV, $E_T^{\rm jet,2} > 6.5$ GeV and $-1 < \eta^{\rm jet} < 2$. The cross sections are measured in the phase space defined by $0.2 < y < 0.55$ and $0.1 < Q^2 < 0.55$, $1.5 < Q^2 < 4.5$, $4.5 < Q^2 < 10.5$, $10.5 < Q^2 < 49.0$ and $49.0 < Q^2 < 10^4$ GeV^2.

The measured triple differential dijet cross sections $d^3\sigma/(dx_\gamma^{\rm obs} dQ^2 d\overline{E}_T^2)$ are shown as a function of $x_\gamma^{\rm obs}$ in figure 3 in different bins of Q^2 and $\overline{E}_T^2$. The LO Herwig predictions using the SaS1D parametrization [10] for the photon PDFs do not describe the absolute cross section of the data. They are therefore normalized to the highest $x_\gamma^{\rm obs}$ bin ($x_\gamma^{\rm obs} > 0.75$) in order to compare the shape of the data with that of the MC predictions. For each $\overline{E}_T^2$ bin, the cross section in the low $x_\gamma^{\rm obs}$ region falls faster with increasing Q^2 than the cross section in the high $x_\gamma^{\rm obs}$ region. For the bins with $Q^2 > \overline{E}_T^2$ the data are well described by the Herwig predictions including only the LO-direct component. In the bins with $Q^2 < \overline{E}_T^2$ the LO-direct component is not enough to describe the data.

The ratio of cross sections $R = \sigma(x_\gamma^{\rm obs} < 0.75)/\sigma(x_\gamma^{\rm obs} > 0.75)$ as a function of Q^2 and for three ranges in $\overline{E}_T^2$ is shown in figure 3. The ratio of the data falls with increasing Q^2 for each range of $\overline{E}_T^2$. These results show the suppression of the virtual photon structure with increasing photon virtuality. The Herwig prediction using SaS1D also falls with increasing Q^2 but underestimates the measured ratio.

[a] $\overline{E}_T$ is the mean transverse energy of the two leading E_T jets.

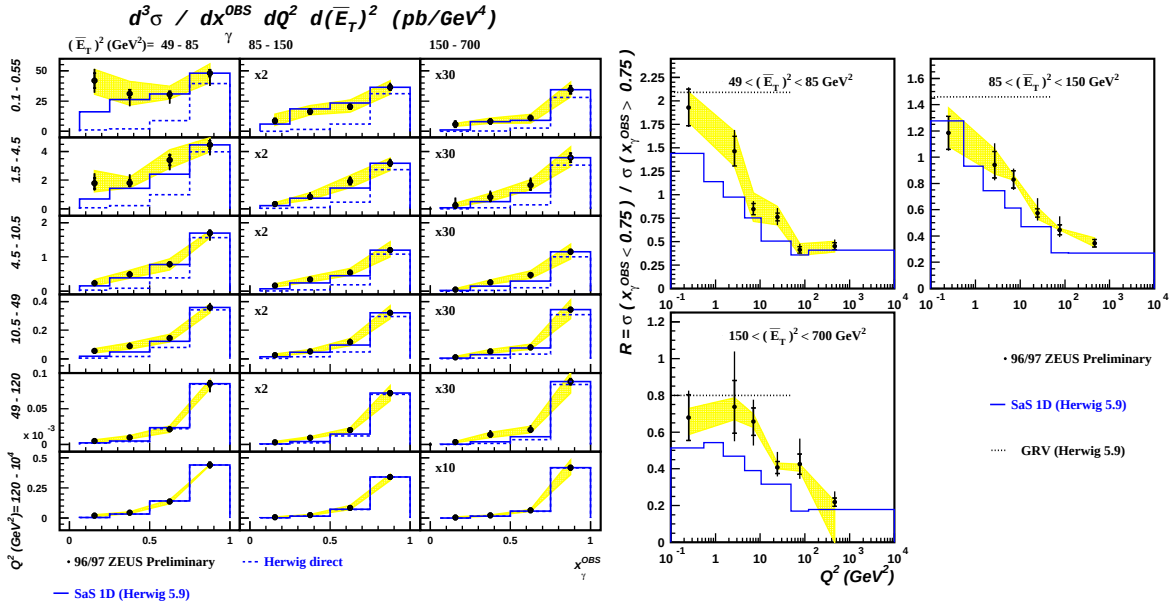

Figure 3: Triple differential cross section $d^3\sigma/(dx_\gamma^{\rm obs} dQ^2 d\overline{E}_T^2)$ as a function of $x_\gamma^{\rm obs}$ for different regions in Q^2 and $\overline{E}_T^2$ (left plot). The ratio of cross sections $R = \sigma(x_\gamma^{\rm obs} < 0.75)/\sigma(x_\gamma^{\rm obs} > 0.75)$ as a function of Q^2 for different ranges in $\overline{E}_T^2$ (right plot). The points represent the measured cross sections with statistical errors (inner error bars) and uncorrelated systematic errors added in quadrature to them (outer error bars). The shaded bands display the uncertainty in the plotted quantities due to that in the jet energy scale.

3 Conclusions

The structure of real and virtual photons has been studied at HERA using dijet production. The use of the data from the real photon measurements in future fits would greatly improve our understanding of the photon PDFs. More thorough studies can be done using the new measurements in the challenging phase space region of virtual photons.

References

[1] ZEUS Collab. M.Derrick et al., *Phys.Lett.* **B348** (1995) 665

[2] H1 Collaboration, *Phys.Lett.* **B483** (2000) 36-48

[3] M. Glück, E. Reya, A. Vogt, *Phys. Rev.* **D46** (1992) 1973
M. Glück, E. Reya, A. Vogt, *Z. Phys.* **C53** (1992) 127

[4] G. D'Agostini, Nucl.Instrum.Methods **A362** (1995) 487

[5] S. Frixione, *Nucl. Phys.* **B507** 295 (1997)
B.W.Harris and J.F.Owens, *Phys. Rev.* **D56** 4007 (1997)
M.Klasen and G.Kramer, *Z.Phys.* **C76** 67 (1997)
M.Klasen, T.Kleinwort and G.Kramer, *Eur.Phys.J.* **C1** 1 (1998)

[6] P.Aurenche, J.Guillet and M.Fontannaz, *Z.Phys.* **C64** (1994) 621

[7] H.L.Lai et al., *Phys.Rev.* **D55** (1997) 1280

[8] G. Corcella, I.G. Knowles, G. Marchesini, S. Moretti, K. Odagiri, P. Richardson, M.H. Seymour and B.R. Webber. *HERWIG6.2* hep-ph/0011363 (2000).

[9] T. Sjöstrand et al. *High-Energy-Physics Event Generation with Pythia6.1* hep-ph/0010017 (2000).

[10] Schüler and Sjöstrand, *Phys.Lett.* **B376** (1996) 193